ASEE AMERICAN SOCIETY FOR ENGINEERING EDUCATION

Paper ID #44746

# Development and Optimization of a 3D-Printed Microfluidic Device with Enhanced Transparency for Bioimaging Applications

**Ana Sofia Aviles Vargas, The University of Texas at San Antonio (Department of Biomedical Engineering and Chemical Engineering)**

Ana Aviles Vargas is the current President of the Society of Hispanic Professional Engineers at the University of Texas at San Antonio (UTSA) and has over a year of experience in a UTSA chemical engineering lab. She also served as a Research and Development Intern at Eli Lilly and Company, contributing valuable insights to the pharmaceutical industry. She is dedicated to promoting diversity and inclusion in engineering, showcasing leadership within the Society of Hispanic Professional Engineers.

**Dr. Gongchen Sun, The University of Texas at San Antonio**

I am an Assistant Professor in the Department of Biomedical Engineering and Chemical Engineering at the University of Texas at San Antonio (UTSA). I obtained my BS in Microelectronics from Peking University in 2012, PhD in Chemical Engineering from University of Notre Dame in 2017, and completed a postdoc training in Biomedical Engineering from Georgia Institute of Technology. My research field is in microfluidics, electrokinetics, systems bioengineering, and innovative engineering education.

Session XXXX

# Development and Optimization of a 3D-Printed Microfluidic Device with Enhanced Transparency for Bioimaging Applications

**Ana S. Aviles Vargas, Gongchen Sun**
Biomedical Engineering and Chemical Engineering Department
The University of Texas at San Antonio

## Abstract

This project, grounded in Biomaterials and Bioinstrumentation courses within Biomedical Engineering, aims to enhance the optical transparency and resolution of microfluidic devices fabricated using low-cost digital light processing (DLP) 3D printing. Prioritizing affordability and accessibility, we modified a commercially available 3D printer (Phrozen Sonic Mini 8K) by substituting the build plate with surface-treated glass slides. These slides underwent surface treatment to effectively modify their hydroxy-group-rich surface with a hydrophobic agent (3-(Trimethoxysilyl)propyl methacrylate (TSMPMA)) under oxygen plasma. Additionally, the z-axis limit switch was adjusted to accommodate the thickness of the glass slide on the build plate. Our method significantly improves transparency and resolution, enabling precise segmentation of micro-scale objects from analyzed images obtained through a microscope. The enhanced optical clarity and microchannel resolution of the device can facilitate imaging and characterization of microparticles, thus paving the way for high-throughput cell sorting applications. This interdisciplinary approach integrates knowledge from core Biomedical Engineering courses, emphasizing applications in cell and bioimaging.

## Introduction

Microfluidic devices consist of microchannels that are either etched or molded into a material. There are various applications for microfluidic devices, including medical diagnostics, molecular separation, cell-based assays, drug encapsulation, etc [1]. Microfluidic devices can be created using different materials, including polymers and glass [2]. The channels typically have dimensions ranging from several tens to hundreds of microns and utilize extremely small quantities of liquid, as small as one nanoliter.

Poly(dimethylsiloxane), also known as PDMS, is one of the most used materials to create microfluidic devices due to its processability through soft lithography (molding). PDMS offers various advantages, including optical transparency, biocompatibility, and the ability to create micron-resolution features [2]. Soft lithography is the technique used to create devices with PDMS. To make PDMS-based microfluidic devices, a master mold of the desired device is created. The mold is employed to produce specific features by casting PDMS onto it and then bonding it to another PDMS slab or a glass slide to complete the device. Some drawbacks of using PDMS include its incompatibility with specific organic solvents, the complex and lengthy fabrication process, and limitations in achieving complex 3-dimensional geometries [3].

In the 1980s, the concept of 3D printing was proposed, leading to the development of various 3D

printing methods, including stereolithography (SLA). Stereolithography utilizes a photopolymerization technique where resin, a photosensitizing liquid, serves as the material [4]. This method involves the layer-by-layer curing of the resin with a focused laser or a digital light printer, allowing the resin to harden [3]. The printing process begins with generating a 3D model in computer modeling software. After creating the model, it is inserted into slicer software, where the print is sliced into layers. Finally, the print is produced by the 3D printer. Stereolithography has gained popularity in the microfluidic community due to its capability to create custom, complex microfluidic systems for various research applications.

Furthermore, digital light processing (DLP) is another common process for resin 3D printing. DLP consists of 3D printing that forms 3D structures through digitalized UV light that solidifies liquid photocurable resin [5]. This technique is known for lower manufacturing costs and greater accessibility due to its increased commercialization. However, this technique has drawbacks, including low transparency even with commercially clear resins, low resolution limiting microchannel size, and a lack of biocompatibility due to potential cytotoxic solvents [6]. Although various commercially available clear resins, such as Formlabs Clear, NOVA 3D Clear Resin, and Phrozen Aqua Clear, are used, the final prints exhibit only slight transparency. This presents challenges for imaging applications and places 3D printed microfluidic devices below PDMS devices.

This study addresses the challenges of creating optically transparent microfluidic devices using accessible DLP 3D printing and provides a comprehensive analysis of how modifications affect the overall transparency and resolution of the printed device. By modifying a DLP printer with a modification of the z-limit switch and creating a smooth build plate using a glass surface treatment, improved transparency is achieved. Two resin materials were studied and compared to understand the changes exhibited by the prints. Additionally, two DLP 3D printers and one SLA 3D printer were utilized to compare the transparency and resolution of the modified printer to a non-modified printer. To quantify transparency, we developed an imaging assay using printed micropillars allowing us to obtain diameter and circularity values from segmentation. The in situ printed micropillars were imaged and analyzed using Image J, where they were segmented and compared to each other to evaluate the transparency of the 3D printed device.

## Methods

### Printer and Resin Selection

Two types of printers were utilized in this study: a DLP-based printer and an SLA-based printer. The first type was the Phrozen Sonic Mini 8K; two of these printers were used. One served as our positive control and underwent all printer modifications, while the other underwent no printer modifications. The modified Phrozen printer is referred to as the 'Modified DLP Printer,' while the unmodified Phrozen printer is referred to as the 'Unmodified DLP Printer.' The second printer type was the Formlabs Form 3+, which served as our negative control and did not undergo any printer modifications. This printer is referred to as the 'Unmodified SLA Printer.' These printers were employed to compare the transparency and resolution of identical prints. It is important to note that the Phrozen Sonic Mini 8K allowed for cross-compatibility with various resins, whereas the Formlabs Form 3+ printer only permitted the use of their resin due to its structural limitations. The resins used in the study included Formlabs Clear Resin and NOVA 3D Clear Resin

## Printer Modifications

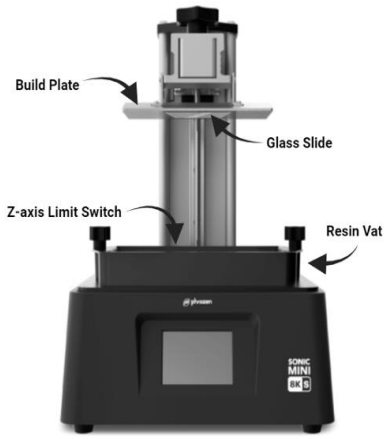


**Figure 1. Phrozen 3D Printer Key Components**

The primary approach to achieving transparency involved making hardware modifications to the utilized 3D printer, the Phrozen Sonic Mini 8K. This 3D printer comprises three main components, as illustrated in Figure 1. These components include the build plate (where the model is printed), the z-axis limit switch (detecting the point at which the build has reached its maximum lowering), and the resin vat containing the resin. The transparency of the print is influenced by light scattering on the rough surfaces of both the build plate and the resin vat, resulting in a decrease in transparency. To address this, a siliconized glass slide was added to the build plate to create a smooth surface. To accommodate the added thickness of the glass slide, a customized capsule, mimicking the thickness of the glass slide, was placed inside the linear stage actuator of the printer to manipulate the z-axis limit switch.

## Glass Surface Treatment

To ensure adherence of the 3D printed model to the glass slide, the glass slides underwent surface treatment to effectively modify their hydroxy-group-rich surface, shown in Figure 2. The glass slide was initially cleaned with isopropyl alcohol and water, followed by drying with pressurized air. Subsequently, the plasma etch wand was employed on the glass slide for approximately one minute and thirty seconds. The treated glass slide was then wrapped in a Kimtech lint-free wipe with the plasma-treated side facing up. Following this, 800uL of a siliconizing agent, 3-(Trimethoxysilyl)propyl methacrylate (TSMPMA), was applied to impart a hydrophobic surface. Once the TSMPMA fully saturated the Kimtech wipe, the wrapped slide was placed in a hot air oven set at 85°C.

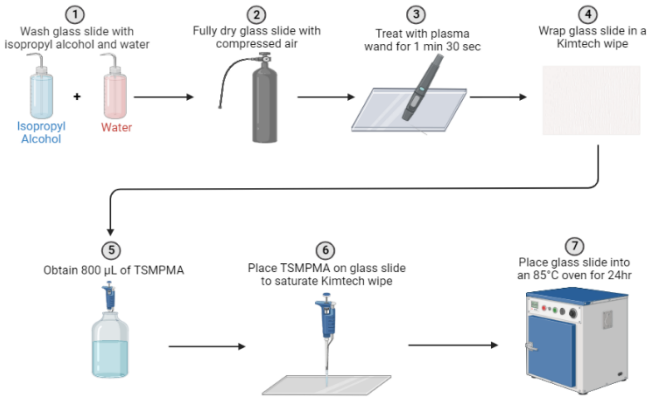


**Figure 2. Surface Treatment Protocol for Glass Slides**

## Transparency characterization and image analysis

To comprehensively assess the transparency of both prints, a microfluidic device incorporating micropillars (1mm in diameter) was fabricated. These prints were infused with yellow fluorescence and subjected to imaging using an ECHO Inverted Microscope. Subsequent analysis in Image J involved segmentation and the evaluation of circularity and area dimensions. This analytical approach facilitated a transparency assessment by analyzing the area gathered from the segmentation. The obtained area was used to calculate the diameter of the micropillar, which was then converted from

microns (µm) to millimeters (mm) to obtain the final result.

## Results and Discussion

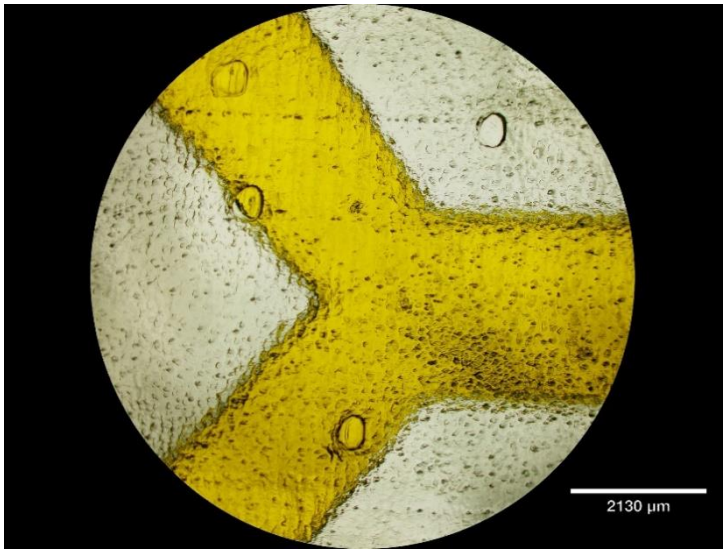


**Figure 3. Negative Control: Unmodified SLA 3D Printed Microchannel**

In Figure 3, a microchannel printed with the unmodified 3D printer is depicted. The microchannel measures 2mm in width and is filled with 1mM of yellow fluorescence. The figure illustrates the rough surface of the print after the post-printing process. The layer-by-layer printing process is evident in the figure during imaging, with irregularities on the print surface, such as small circular holes, observable. These holes result from the implementation of supports on the print to ensure correct printing. The lack of transparency contributes to a blurring effect, thereby limiting the ability to measure the microchannel or any particles within it. This limitation restricts the potential applications of this device.

In Figure 4, a microchannel printed with the modified DLP 3D printer is presented. The microchannel measures 1mm in width and is filled with blue dye. This figure highlights the optical transparency achieved with the modified DLP 3D printer. The ability to observe bubbles created by the influx of dye further underscores the clarity of the print. Imaging reveals a lack of visibility of surface roughness compared to Figure 3. It is evident that the condition of the build plate significantly influences the overall transparency of the device. Moreover, there is minimal blurring on the channel; the starting and ending points of the channel are clearly discernible. This observation emphasizes the capability to accurately measure particles or cells within this microchannel.

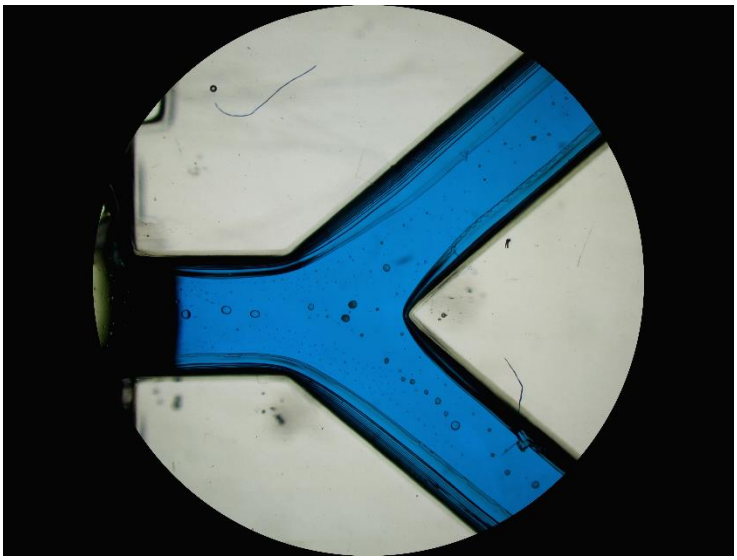

**Figure 4. Positive Control: Modified DLP 3D Printed Microchannel**

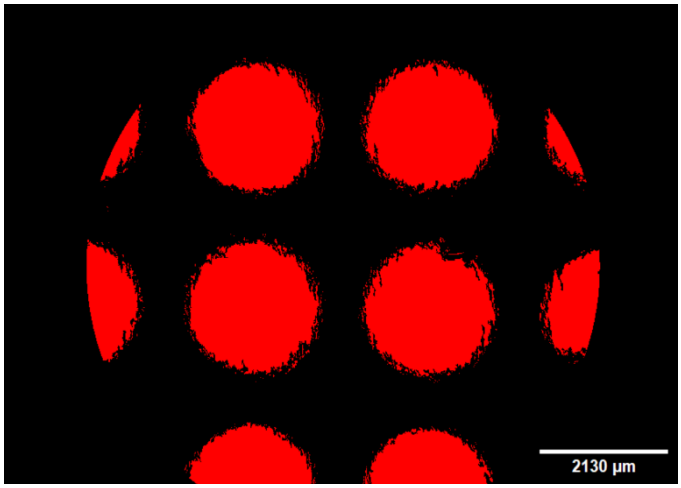


**Figure 5. Segmentation results of from the Unmodified SLA 3D printed micropillars obtained through Image J analysis, showcasing the detailed identification and delineation of individual structures for further quantitative assessment.**

Segmentation of each image was performed using Image J software, where it identified the structure through the contrast between the fluorescence and the structure. In Figure 5, the segmentation of the unmodified SLA 3D printer (Formlabs 3+) is depicted. The figure reveals irregularities throughout each cylindrical microstructure. There are also areas within the structure that contain holes within the identified circle; this is attributed to the lack of transparency in the print, where rough surfaces are evident during imaging, causing discrepancies in segmentation. Additionally, not all microstructures fit within the image, leading to them being cut off and affecting the data gathered from segmentation. Therefore, the micropillars that are cut off are excluded from the data**.**

In Figure 6, the segmentation of an unmodified DLP printer (Phrozen Unmodified) is depicted. It is evident that the device overall lacked clarity, resulting in inadequate segmentation. This figure also illustrates the printer's standard printing resolution without any modifications. The surface appears rough, leading to reduced clarity when imaging the micropillars with fluorescence.

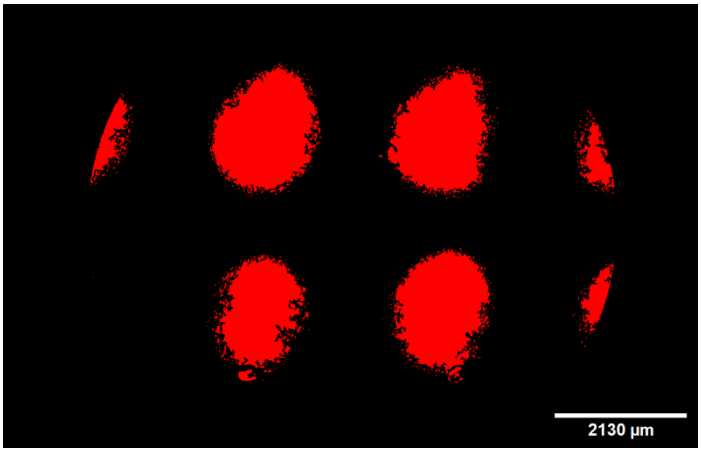


**Figure 6. Segmentation outcomes of micropillars printed with the unmodified DLP 3D printer were analyzed using ImageJ. The figure illustrates a lack of transparency, resulting in reduced clarity.**

In Figure 7, the segmentation of the modified DLP 3D printer is presented. A clear distinction between the modified and unmodified segmentation is evident. The irregularities seen in Figure 6 are minimal. Consequently, the software accurately identifies the shape of the micropillar and segments it correctly. In the segmentation of the modified DLP printer, the shape of the micropillar is visibly clear to the naked eye, enhancing the precision of diameter and circularity results obtained through the software. To maintain accuracy, micropillars that were cut off during imaging were excluded from the dataset. Comparing Figure 7 to Figure 6, it is clear the overall modification of the printer allows for improved clarity and transparency. This further emphasizes the impact that the modification has on the overall printed micropillars.

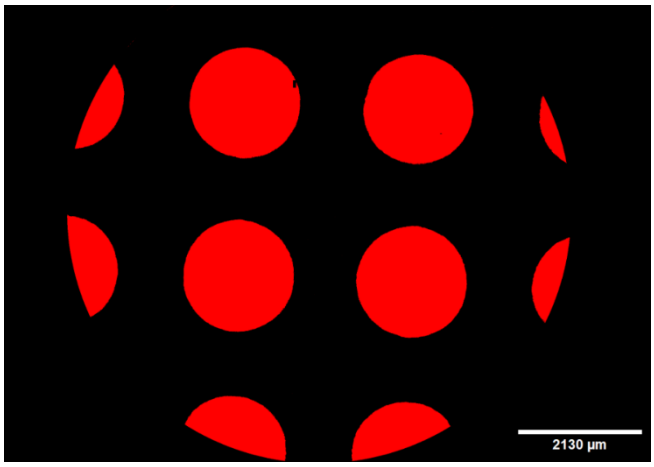


**Figure 7. Segmentation outcomes of micropillars printed with the modified DLP 3D printer, analyzed using Image J. The figure illustrates precise identification and segmentation of individual micropillars, highlighting the impact of printer modifications on structural clarity.**

In Figure 8, the diameters obtained from the analysis software are presented, providing a clear comparison between the diameters obtained through the segmentation of both the unmodified and modified printers. The modified DLP 3D printer exhibits greater consistency among the analyzed microstructures when comparing the diameters. In contrast, the unmodified DLP 3D printer shows greater inconsistency across the measured microstructures, with diameters ranging from 0.14 to 0.19 mm less than the original diameter of 1 mm. This variability highlights the lack of transparency in the unmodified DLP 3D printer, leading to a lower range of diameters due to challenges in proper segmentation. Conversely, the modified 3D printer demonstrates a narrower range, from 0.94 mm to 0.96 mm, with a repeatability of the diameter at 0.95 mm. This underscores the reproducibility of the diameter across the modified DLP 3D printer, showcasing its consistency.

When comparing the unmodified SLA printer, there is also increased consistency in diameters ranging from 1.01 to 1.03 mm. This showcases the quality of the overall resolution. Due to the use of a laser in the printer, it allows for finer details to be created, therefore generating a micropillar closer to the original desired diameter of 1 mm. Additionally, the smaller range between diameters indicates increased transparency, facilitated by accurate segmentation of the micropillars and proper analysis of the structures. Although the diameter results presented by the unmodified Formlabs 3+ SLA printer were closer to the actual diameter of the micropillar, it is to be noted that the printer is ten times the value of the modified Phrozen DLP printer, therefore allowing for more precise details.

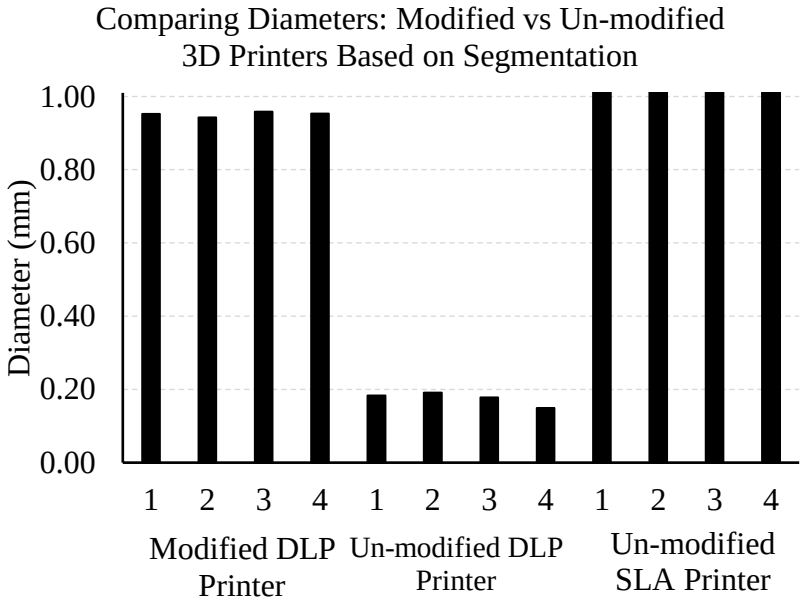


**Figure 8. A comparative analysis of diameters obtained through segmentation of micropillars from both unmodified and modified 3D printers. The graph illustrates the differences in diameter measurements, emphasizing the impact of printer modifications on the dimensional characteristics of the printed micropillars.**

In Figure 9, the comparison of circularity between both printers is depicted. The software calculates

circularity using the equation: $Circularity = \frac{4\pi \times Area}{Perimeter^2}$

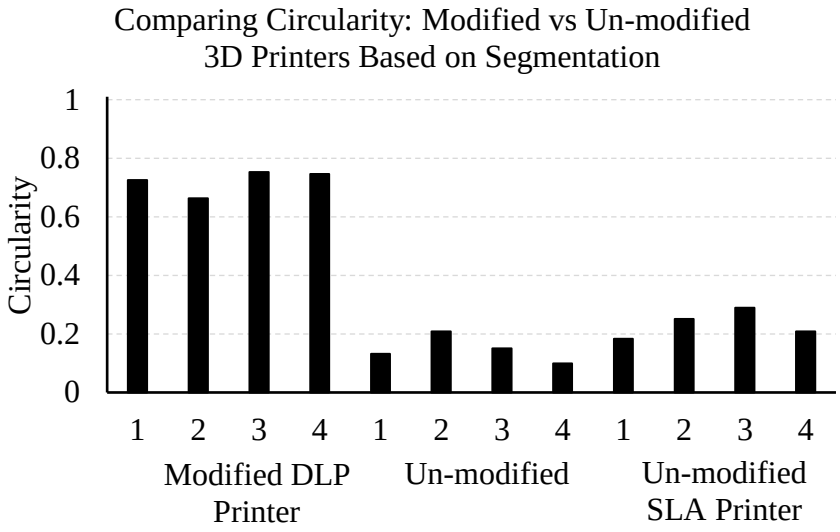


**Figure 9. A comparison of circularity between unmodified and modified 3D printers, revealing differences in the geometric shapes of printed micropillars. Circularity, a metric in Image J, measures how closely an object resembles a perfect circle, with higher values indicating greater circularity and more precise segmentation of microstructures.**

It is evident that there is greater circularity within the modified DLP printer when comparing the circularity values to the other 3D printers. The figure illustrates the range of circularity of the modified DLP 3D printer to be from 0.66 to 0.75, while the other printers exhibit a circularity under 0.29. This further emphasizes the overall improved transparency of the micropillars with printer modifications. The comparison of Figures 5, 6, and 7 shows that the micropillars printed with the modified DLP 3D printer have greater circularity.

## Summary and Conclusions

Using the data gathered through this study, we can further improve the printing methods of microfluidic devices with both commercially available resins and 3D printers. We can address the challenges associated with 3D printing of microfluidic devices using resin, with a specific focus on enhancing transparency and resolution. The limitations of commercially available clear resins, such as Formlabs clear and NOVA 3D clear resin, were acknowledged, emphasizing the need for improvements in imaging applications. By modifying specific aspects of a 3D DLP printer, including the incorporation of surface-treated glass slides and adjustments to the z-axis switch, we aimed to overcome these challenges in a cost-effective manner. It's worth noting that the SLA printer, due to its inability to modify the z-axis, presents constraints in incorporating treated glass surfaces, which are crucial for enhancing transparency. Although creating a glass build plate could be an area to explore, it would increase the overall cost, contradicting our aim to develop a cost-effective solution for transparent 3D printed devices.

Our findings revealed an enhancement in transparency in the modified 3D DLP printer, showcasing the effectiveness of our approach in addressing the limitations of current 3D printing methods. The study not only contributes to the advancement of microfluidic device fabrication but also emphasizes the importance of accessibility and affordability in the development of innovative solutions. The comprehensive analysis of two resin materials and the comparison between modified and unmodified printers demonstrated the efficacy of our approach. The enhanced transparency observed in the modified printer emphasizes the potential of our method in overcoming the limitations of current 3D

printing techniques.

Our study contributes to providing an affordable and accessible solution for producing transparent, high-resolution 3D-printed microfluidic devices. The implications of our findings extend towards advancements in biomedical applications, particularly in imaging technologies. This work underscores the interdisciplinary nature of our approach, integrating principles from core courses in Biomedical Engineering. Moving forward, our research will delve into exploring the reproducibility of generating a cross-compatible resin. This resin aims to enhance resolution while simultaneously improving the overall transparency of the devices. Additionally, we will investigate the application of our method in designing microfluidic devices tailored for high-throughput cell sorting and other bioimaging applications.

## Acknowledgment

We acknowledge the support from the UTSA Startup Fund to G.S. Additionally, I am thankful for being awarded the Klesse Undergraduate Research Scholarship, which provided essential support during this study.

## References


1. Urrios, A., Parra-Cabrera, C., Bhattacharjee, N., Gonzalez-Suarez, A. M., Rigat-Brugarolas, L. G., Nallapatti, U., Samitier, J., DeForest, C. A., Posas, F., Garcia-Cordero, J. L., & Folch, A. (2016). 3D-printing of transparent bio-microfluidic devices in PEG-DA. Lab on a Chip, 16(12), 2287–2294. https://doi.org/10.1039/C6LC00153J
2. Nielsen, J. B., Hanson, R. L., Almughamsi, H. M., Pang, C., Fish, T. R., & Woolley, A. T. (2020). Microfluidics: Innovations in Materials and Their Fabrication and Functionalization. Analytical Chemistry, 92(1), 150–168. https://doi.org/10.1021/acs.analchem.9b04986
3. Quan, H., Zhang, T., Xu, H., Luo, S., Nie, J., & Zhu, X. (2020). Photo-curing 3D printing technique and its challenges. Bioactive Materials, 5(1), 110–115. https://doi.org/10.1016/j.bioactmat.2019.12.003
4. Schittecatte, L., Geertsen, V., Bonamy, D., Nguyen, T., & Guenoun, P. (2023). From resin formulation and process parameters to the final mechanical properties of 3D printed acrylate materials. MRS Communications, 13(3), 357–377. https://doi.org/10.1557/s43579-023-00352-3
5. Shahrubudin, N., Lee, T. C., & Ramlan, R. (2019). An Overview on 3D Printing Technology: Technological, Materials, and Applications. Procedia Manufacturing, 35, 1286–1296. https://doi.org/10.1016/j.promfg.2019.06.089
6. LFritschen, A., Bell, A. K., Königstein, I., Stühn, L., Stark, R. W., & Blaeser, A. (2022). Investigation and comparison of resin materials in transparent DLP-printing for application in cell culture and organs-on-a-chip. Biomaterials Science, 10(8), 1981–1994. https://doi.org/10.1039/D1BM01794B



ANA S. AVILES VARGAS

Ana Aviles Vargas is a Biomedical Engineering major with a concentration in Biomechanics at the University of Texas at San Antonio. Currently serving as the president of the Society of Hispanic Professional Engineers (SHPE). Ana was previously a research and development intern at Eli Lilly and Company, working on a high throughput screening assay for oligonucleotide delivery platforms. With a profound interest in the neurodegenerative disease sector, she aspires to pursue a Ph.D. in bioengineering. Ultimately, she aims to bridge academia and industry, contributing to the development of innovative therapies for neurodegenerative diseases.

GONGCHEN SUN

Gongchen Sun is an Assistant Professor in the Department of Biomedical Engineering and Chemical Engineering at the University of Texas at San Antonio (UTSA). Gongchen obtained his BS in Microelectronics from Peking University in 2012, PhD in Chemical Engineering from University of Notre Dame in 2017, and completed a postdoc training in Biomedical Engineering from Georgia Institute of Technology. His research field is in microfluidics, electrokinetics, systems bioengineering, and innovative engineering education.